Dash Waves in a Reaction-Diffusion System

Vladimir K. Vanag and Irving R. Epstein

Department of Chemistry and Volen Center for Complex Systems, MS 015, Brandeis University, Waltham, Massachusetts 02454-9110

(Received 25 July 2002; published 3 March 2003)

Patterns in reaction-diffusion systems generally consist of smooth traveling waves or of stationary, discontinuous Turing structures. Hybrid patterns that blend the properties of waves and Turing structures have not previously been observed. We report observation of dash waves, which consist of wave segments regularly separated by gaps, moving coherently in the Belousov-Zhabotinsky system dispersed in water-in-oil microemulsion. Dash waves emerge from the interaction between excitable and pseudo-Turing-unstable steady states. We are able to generate dash waves in simulations with simple models.

DOI: 10.1103/PhysRevLett.90.098301 PACS numbers: 82.40.Ck, 02.70.Uu, 68.05.Gh, 82.33.Nq

The discovery of chemical waves in the Belousov-Zhabotinsky (BZ) reaction [1] provided a powerful impetus for studying pattern formation in chemical and biological systems. A very different class of patterns, stationary Turing structures [2], were found experimentally 20 years later in another chemical system, the chlorite-iodide-malonic acid reaction [3]. Efforts to find new patterns and even new principles of pattern formation are expanding [4–7], with most recent approaches utilizing external forcing and/or global feedback. Finding new "natural" patterns in autonomous systems remains an important and challenging problem.

Recently, a new class of chemical waves, packet waves [8], which include antispirals [9], was discovered in the BZ system dispersed in aerosol OT (AOT) water in oil microemulsion (BZ-AOT system). Turing structures and trigger waves were also found in that system [10]. The wide variety of patterns in the BZ-AOT system arises from the very different diffusion coefficients of molecules soluble in the oil and in the aqueous phases. The presence of molecules with different diffusion coefficients is a ubiquitous phenomenon in biological systems, where molecular weights may span several orders of magnitude and diffusion may be facilitated by membranes, filaments, or other structural elements. Therefore the BZ-AOT system serves as an excellent model system for probing new patterns potentially important in living systems.

A thermodynamically stable AOT microemulsion consists of nanometer-sized water droplets dispersed in a continuous oil (octane) phase [11]. Each droplet is surrounded by a surfactant (AOT) monolayer. The polar BZ reactants reside almost exclusively in the water droplets and diffuse slowly, with the diffusion coefficient of entire droplets [12]. During the course of the BZ reaction, bromine, which is nonpolar, is produced in the water droplets and diffuses into the oil phase and back to the droplets. Bromine diffuses rapidly through the oil phase and inhibits the BZ reaction by generating bromide ion. When the radius of the droplets R and the volume fraction ϕ_d of the dispersed phase (water + surfactant) as well as the concentrations of the BZ reactants are varied, the spatially extended BZ-AOT system exhibits a variety of patterns [9,10]. A new type of pattern, dash waves (Fig. 1), occurs in a narrow range of R, ϕ_d, and chemical composition.

Experiments were initiated by mixing two stock microemulsions, each having the same size and concentration of water droplets ($\phi_d = 0.55$, $R = 0.17\omega$ nm, $\omega \equiv [H_2O]/[AOT] = 15$). One solution contained H_2SO_4 and malonic acid, the other ferroin and $NaBrO_3$. A small volume of the reactive BZ-AOT microemulsion was sandwiched between two flat optical windows. The gap between the windows was determined by the thickness h

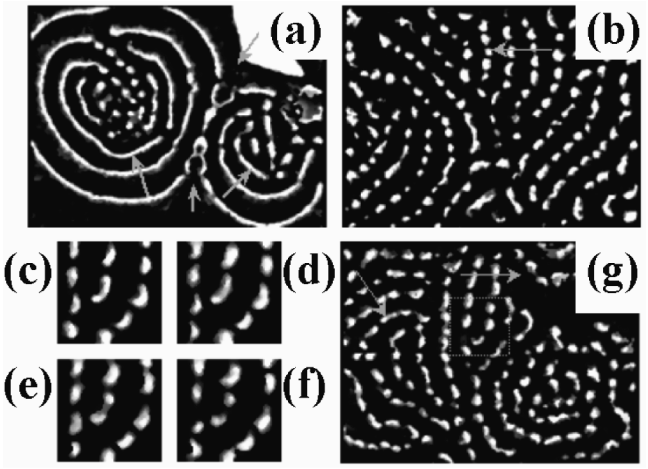

FIG. 1. Dash waves in the BZ-AOT system. Snapshots (b)–(g) are taken, respectively, 1800, 935, 940, 945, 950, and 1000 s after snapshot (a). Dotted square in (g) shows position of snapshots (c)–(f). Large rhomblike white spot in (a) is fast propagating phase wave. Gray levels quantify [ferroin], with white corresponding to minimum and black to maximum. Arrows show general direction of wave propagation. Size (mm × mm) for (a), (b), (g) 2.54 × 1.88; for (c–f) 0.53 × 0.53. Concentrations: [MA] = 0.3 M, $[H_2SO_4] = 0.2$ M, $[NaBrO_3] = 0.23$ M, [ferroin] = 4 mM. Wavelength λ_1 is about 0.19 mm; wave velocity is 1.5–2 μm/s.

(= 0.1 mm) of an annular Teflon gasket with inner and outer diameters of 20 and 47 mm, respectively. Patterns were observed at 23 °C for about 1 h through a microscope equipped with a digital CCD camera connected to a personal computer. The reaction area was illuminated through a 500 nm interference filter.

Initially, fast phase waves emerge and evolve into continuous trigger waves. After 10–20 min, when bulk oscillations cease in a reference BZ-AOT system of the same composition in a continuously stirred tank reactor, the mode of transformation of phase waves into trigger waves changes. When a phase wave approaches the region between two wave basins, small islands of local activity materialize in front of the wave and give rise to circular waves [center of Fig. 1(a)]. These waves do not, as one might expect, merge to generate a flat front. Instead, continuous ripple waves and then dash waves [Figs. 1(b) and 1(g)] emerge and occupy the entire area. After 20–30 min, the dash waves give way to "bubbles," small circular waves that emerge randomly, grow slightly while their centers remain fixed, and then vanish without colliding with other bubbles. The bubbles are succeeded by standing waves, and finally, after 1–1.5 h, all patterns disappear, as they must in a closed system.

A typical pattern is composed of groups of concave dash waves moving in parallel and separated by wavelength λ_1. Each wave consists of small convex segments (dashes) with characteristic length l_2, which is slightly smaller than λ_1. A few points act as turning points or defects, where dash waves branch and change their direction of propagation. At such points, the dash closest to the turning point first increases in length and then splits into two new dashes [Figs. 1(c)–1(f)].

A lateral instability leading to ripple (or cellular) fronts in a system with cubic autocatalysis was predicted by Horváth *et al.* [13] and was found experimentally in the iodate-arsenous acid reaction [14]. With such lateral instabilities, the characteristic length of the front nonuniformity (cellular structure) is not intrinsic to the chemical system, but rather depends upon the total width of the medium. Our experiments and theory (below) show that the length of the dashes depends only on the chemical parameters, and not on the geometry, of our reaction-diffusion system. Ripple fronts of outwardly propagating spiral waves have also been found in the BZ reaction [15]. Hagberg and Meron [16] have shown in a FitzHugh-Nagumo type model that a transverse instability can lead to an unstable array of moving spots, which ultimately evolves to spiral chaos.

Dash waves arise only in experiments with "fresh" microemulsions, used within several hours of mixing aqueous solutions of the BZ reagents with an octane solution of AOT. Day-old microemulsions with the same concentrations give a variety of other patterns [9,10], but not dash waves. Light scattering experiments reveal that the distribution of droplet radii in a newly prepared stock microemulsion [this procedure takes approximately 1 h of intensive stirring, because of the high concentrations of salt ($NaBrO_3$) and sulfuric acid] is bimodal, with one peak at 2 nm and another at 20 nm (Fig. 2). The two peaks slowly merge, and a monodisperse droplet distribution centered at 3.6 nm is established within one to two days. Thus, at least two relatively stable subsystems of the BZ-AOT system with different diffusion coefficients and even different rates of reaction (both quantities depend on the size of the water droplets [11,17]) can interact in a fresh microemulsion. By "relatively stable" we mean that the distribution of droplet radii is essentially constant during our one-hour experiment.

To gain insight into how dash waves might arise in such a system, we consider the problem of two coupled subsystems (droplets of different sizes) distributed in space. Starting from a two-variable Oregonator-type model [18], we obtain the following equations for model A:

$$\begin{aligned}
\partial x_1/\partial\tau &= (1/\varepsilon_1)[x_1 - x_1^2 + f_1 z_1(q_1 - x_1)/(x_1 + q_1)] \\
&\quad - \phi k_x(x_1 - x_2) + D_{x1}\Delta x_1, \\
\partial x_2/\partial\tau &= (1/\varepsilon_2)[x_2 - x_2^2 + f_2 z_2(q_2 - x_2)/(x_2 + q_2)] \\
&\quad - k_x(x_2 - x_1) + D_{x2}\Delta x_2, \\
\partial z_1/\partial\tau &= x_1 - z_1 - \phi k_z(z_1 - z_2) + D_{z1}\Delta z_1, \\
\partial z_2/\partial\tau &= x_2 - z_2 - k_z(z_2 - z_1) + D_{z2}\Delta z_2,
\end{aligned} \tag{1}$$

where x and z are dimensionless concentrations of activator ($HBrO_2$) and oxidized catalyst (ferriin), respectively. Subscripts 1 and 2 refer to the two subsystems; k_x and k_z are rate constants for x- and z-mass exchange between subsystems, respectively; ϕ ($= V_2/V_1$) is the ratio of volumes of the subsystems. Diffusion coefficients of z species (z is the inhibitor in the two-variable Oregonator model) are chosen larger than those of x species to account for the fast diffusivity of the inhibitor Br_2 in the oil phase. In earlier work on the BZ-AOT

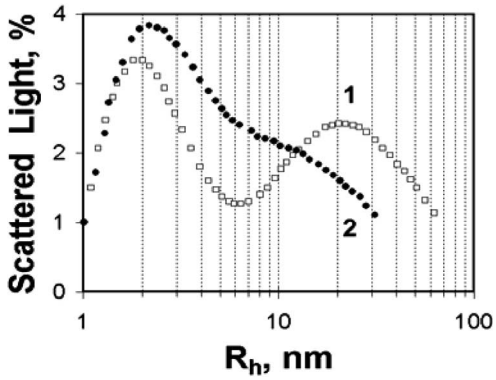

FIG. 2. Distribution of radii of water nanodroplets. Curves 1 and 2 were obtained in light-scattering experiments for fresh and one day old microemulsions ($\omega = 15$, $\varphi_d = 0.55$), respectively, loaded with H_2SO_4 (0.4 M) and MA (0.6 M).

system we have used an Oregonator model augmented with a fast-diffusing activator [10] or with both a fast-diffusing activator and inhibitor [8]. Here we employ only a fast-diffusing inhibitor without either a slow-diffusing inhibitor or a fast-diffusing activator (the latter is important for wave instability but not for Turing instability). This choice simplifies the model but shrinks the domain of stability where dash waves are found.

In a range of parameters, system (1) generates three homogeneous steady states, one of which ("middle") is always an unstable saddle. The other two steady states may have a variety of characters. We shall be particularly interested in the case where one, which we designate the "low" steady state because it has a lower concentration of x_2, is stable but excitable, and the other, "high" state possesses an eigenvalue λ such that $\mathrm{Re}(\lambda) > 0$ at wave number $k = 0$ and for some range of k has an eigenvalue such that $\mathrm{Im}(\lambda) = 0$ and $\mathrm{Re}(\lambda) > 0$, with a maximum in $\mathrm{Re}(\lambda)$ at $k = k_0$ (Fig. 3). We refer to this behavior as a pseudo-Turing (PT) instability. Such an instability differs significantly from the usual Turing instability, in which $\mathrm{Re}(\lambda) < 0$ at $k = 0$; in particular, the uniform steady state of a PT-unstable system is unstable to homogeneous perturbations. When the parameters are chosen so that the PT instability arises, simulation of system (1) can yield patterns resembling dash waves [Fig. 4(a)].

Classical Turing patterns [3] are stationary structures [2]. The motion of the dashes that develop out of the PT instability arises from the dual nature of dash waves. On the one hand, the medium is excitable and supports propagation of trigger waves. A superthreshold perturbation switches the system from the "low," excitable steady state to an unstable ("max") state with a large concentration of activator essentially determined by the autocatalytic step and its termination reaction [the first two terms in the second equation of (1)], i.e., by $x_2 - x_2^2 \cong 0$. The max state relaxes not to the initial low state, as it would in a simple trigger wave, but rather to the high Turing-unstable steady state. Because of the PT instability, decay of the max state is not spatially uniform. Interplay between the max and high states leads to emergence of one-dimensional Turing patterns composed of dashes (max state) and gaps (high state) along a dash wave with a characteristic length $2\pi/k_0$. Dash waves are then a strongly nonlinear phenomenon. The inhibitor, which is generated primarily in the dashes, diffuses faster than the activator and suppresses the autocatalytic reaction in the gaps. Immediately behind a dash wave, there is a zone of high steady state, which is unstable because $\mathrm{Re}(\lambda) > 0$ and therefore switches back to the stable low steady state. The max state in the dashes serves as a superthreshold perturbation for the low excitable state and gives rise to local waves, thus leading to propagation of the (one-dimensional) Turing pattern. The concentrations of activator and inhibitor in the high and low steady states are relatively close to each other but significantly smaller than in the max state. Thus, while the gaps and

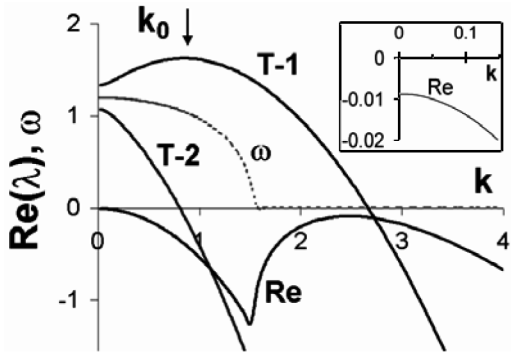

FIG. 3. Dispersion curves for model A with parameters: $q_1 = 0.01$, $q_2 = 0.003$, $f_1 = 2.4$, $f_2 = 1.25$, $\varepsilon_1 = 0.18$, $\varepsilon_2 = 0.13$, $\phi = 1$, $k_x = 0.9$, $k_z = 5$, $D_{x1} = 0.1$, $D_{x2} = 0.38$ (emergence of dash waves is nearly independent of D_{x1} in the range 0.07–0.5, but strongly dependent on D_{x2}), $D_{z1} = 1$, $D_{z2} = 0.7$. Curves T-1 and T-2 are real eigenvalues ($\omega = 0$ at all k), corresponding to the "high" steady state with pseudo-Turing instability; curves Re and ω correspond to the excitable steady state (curve ω is the imaginary part of the eigenvalue divided by 1.6). Maximum of curve T-1 at $k = k_0$ is marked by arrow. Behavior of curve Re near the onset is shown in the inset.

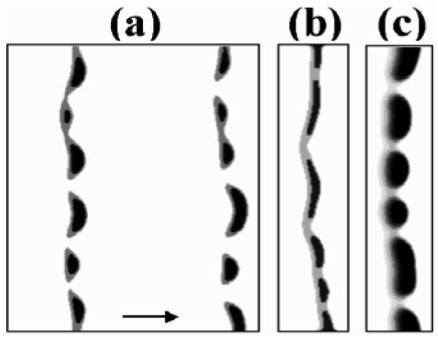

FIG. 4. Dash waves in (a) coupled Oregonator model A; (b) single Oregonator model B; and (c) Gray-Scott model GS. Waves develop from initial perturbation of a thin vertical stripe at the left boundary (with excitable steady state elsewhere) and correspond to time after perturbation $t = 23$ in (a),(b) and to $t = 1000$ in (c). Relative position of dashes can change slightly during wave propagation. Gray levels quantify $[x_1] + [x_2]$ for model A and $[x]$ (activator) for B and GS models, with black corresponding to maximum and white to minimum [up to 50% of initial gray levels are transformed to minimum to increase contrast in (a) and (b)]. Wavelength λ_T of pseudo-Turing instability (calculated by linear stability analysis as $\lambda_T = 2\pi/k_0$) and averaged l_2 (measured from snapshots): 6.98 and 7 for (a), 2.32 and 2.3 for (b), and 19.62 and 19.6 for (c). Vertical size of (a), (b), and (c): 30, 17, and 150, respectively. Model parameters: [(a), model A] as in Fig. 3; [(b), model B] $q = 0.005$, $f = 1.31$, $\varepsilon = 0.02$, $D_x = 0.22$, $D_z = 1$, $k_{\mathrm{ex}} = 1.2$, $z_0 = 0.03$; [(c), model GS] $k_2 = 0.0136$, $F = 0.0011$, $D_x = 0.15$, $k_1 = y_0 = D_y = 1$.

the zones between dash waves in our experiments appear identical, they actually correspond to different steady states.

If the above analysis is correct, then it should be possible to generate dash waves in a simpler two-variable activator-inhibitor model where a feed term is introduced in place of the bimodal distribution of droplets in our batch experiment as the source of multiple steady states. A single subsystem of (1) can be transformed into model B:

$$\partial x/\partial t = (1/\varepsilon)[x - x^2 - fz(x - q)/(x + q)] + D_x \Delta x,$$
$$\partial z/\partial t = x - z + k_{\mathrm{ex}}(z_0 - z) + D_z \Delta z, \tag{2}$$

where the feed term $k_{\mathrm{ex}}(z_0 - z)$ has been added to the Oregonator model. For appropriate parameter choices, the small parameter ε is responsible for the excitability of the low steady state, and the condition $D_x \ll D_z$ results in PT instability of the high steady state. For a very narrow range of parameters this model gives waves intermediate in character between unbroken ripple waves and dash waves [Fig. 4(b)].

Clearer examples of dash waves [Fig. 4(c)] are obtained in the Gray-Scott model (GS) [19–21] with parameters that yield an excitable stable steady state and a PT instability for a second steady state (the dispersion curves for the PT-unstable steady state are similar to curves T-1 and T-2 in Fig. 3):

$$\partial x/\partial t = k_1 x^2 y - (F + k_2)x + D_x \Delta x,$$
$$\partial y/\partial t = -k_1 x^2 y + F(y_0 - y) + D_y \Delta y. \tag{3}$$

In all three models, A, B, and GS, l_2, the length of dashes, is determined by the characteristic wave number k_0 of the PT instability, $l_2 \cong 2\pi/k_0$. In both the Oregonator and Gray-Scott models, dash waves require a delicate balance between the diffusion ratio D_x/D_z (D_x/D_y) and the time scale ratio [ε for the Oregonator and $F/(F + k_2)$ for the Gray-Scott model]. A small increase in D_x/D_z (or a decrease in ε) leads to smooth ripple waves. A small decrease in D_x/D_z (or an increase in ε) leads to "bubbles," like those found in the later stages of our experiments, or to Turing patterns or stable dissipative solitons, like those found previously in the Gray-Scott model [20]. PT instability and excitability are necessary, but not sufficient, conditions for dash waves. It may be necessary to take into account more subtle effects like dash curvature and its influence on dash-wave velocity [22].

Adding to any of these models a second fast-diffusing inhibitor, analogous to the fast-diffusing Br_2 in the BZ-AOT system, extends the parameter range where dash waves exist. A similar approach has been utilized to stabilize moving spots in a two-variable FitzHugh-Nagumo-like activator-inhibitor model [23].

We expect that dash waves will be found in living systems, where multiple steady states, species with extremely different diffusion coefficients, waves, and Turing-like patterns are frequently encountered. Among recent reports of new patterns formed by microorganisms [24] are some [25] that resemble dash waves.

This work was supported by the Chemistry Division of the National Science Foundation. We thank Amy Milne for assistance in conducting the light scattering experiments.

[1] A. N. Zaikin and A. M. Zhabotinsky, Nature (London) **225**, 535 (1970).
[2] A. M. Turing, Philos. Trans. R. Soc. London, Ser. B **237**, 37 (1952).
[3] V. Castets, E. Dulos, J. Boissonade, and P. De Kepper, Phys. Rev. Lett. **64**, 2953 (1990).
[4] M. Kim *et al.*, Science **292**, 1357 (2001).
[5] I. Z. Kiss, Y. Zhai, and J. L. Hudson, Science **296**, 1676 (2002).
[6] T. Sakarai, E. Mihaliuk, F. Chirila, and K. Showalter, Science **296**, 2009 (2002).
[7] J. Wolff, A. G. Papathanasiou, I. G. Kevrekidis, H. H. Rotermund, and G. Ertl, Science **294**, 134 (2001).
[8] V. K. Vanag and I. R. Epstein, Phys. Rev. Lett. **88**, 088303 (2002).
[9] V. K. Vanag and I. R. Epstein, Science **294**, 835 (2001).
[10] V. K. Vanag and I. R. Epstein, Phys. Rev. Lett. **87**, 228301 (2001).
[11] T. K. De and A. Maitra, Adv. Colloid Interface Sci. **59**, 95 (1995).
[12] L. J. Schwartz, C. L. DeCiantis, S. Chapman, B. K. Kelley, and J. P. Hornak, Langmuir **15**, 5461 (1999).
[13] D. Horvath, V. Petrov, S. K. Scott, and K. Showalter, J. Chem. Phys. **98**, 6332 (1993).
[14] D. Horvath and K. Showalter, J. Chem. Phys. **102**, 2471 (1995).
[15] M. Markus, G. Kloss, and I. Kusch, Nature (London) **371**, 402 (1994).
[16] A. Hagberg and E. Meron, Phys. Rev. Lett. **72**, 2494 (1994).
[17] V. K. Vanag and I. Hanazaki, J. Phys. Chem. **100**, 10 609 (1996).
[18] J. P. Keener and J. J. Tyson, Physica (Amsterdam) **21D**, 307 (1986).
[19] P. Gray and S. K. Scott, Chem. Eng. Sci. **38**, 29 (1983).
[20] C. B. Muratov and V. V. Osipov, Eur. Phys. J. B **22**, 213 (2001).
[21] J. E. Pearson, Science **261**, 189 (1993).
[22] V. S. Zykov, A. S. Mikhailov, and S. C. Muller, Phys. Rev. Lett. **81**, 2811 (1998).
[23] C. P. Schenk, M. Or-Guil, M. Bode, and H.-G. Purwins, Phys. Rev. Lett. **78**, 3781 (1997).
[24] E. Ben-Jacob, I. Cohen, and H. Levine, Adv. Phys. **49**, 395 (2000).
[25] E. O. Budrene and H. C. Berg, Nature (London) **376**, 49 (1995).